Lyapunov-based Model Predictive Control of Particulate Processes Subject to Asynchronous Measurements

Jinfeng Liu*, David Muñoz de la Peña, Panagiotis D. Christofides*, James F. Davis***

(Received: 16 August 2007; in revised form: 28 September 2007; accepted: 29 October 2007)

DOI: 10.1002/ppsc.200800030

Abstract

This work focuses on state feedback, model predictive control of particulate processes subject to asynchronous measurements. A population balance model of a typical continuous crystallizer is taken as an application example. Three controllers, i.e., a standard model predictive controller and two recently proposed Lyapunov-based model predictive controllers, are applied to stabilize the crystallizer at an open-loop, unstable steady-state in the presence of asynchronous measurements. The stability and robustness properties of the closed-loop system under the three predictive controllers are compared extensively under three different assumptions on how the measurements from the crystallizer are obtained.

Keywords: crystallization processes, input constraints, model reduction, population balance models, predictive control

1. Introduction

Particulate processes play a key role in the manufacturing of many important products. Some examples include the crystallization of proteins for pharmaceutical applications, the emulsion polymerization for the production of latex, and titania powder aerosol reactors used in the production of white pigments. It is now widely recognized that particulate processes present a number of processing challenges, which are not encountered in gas-phase or liquid-phase processes. One of these challenges is the operation of a particulate process in a way that it consistently makes products with a desired particle size distribution (PSD), which is an important quality index of a particulate product, e.g., the shape of the crystal size distribution in crystallization processes strongly affects crystal function and downstream processing such as filtration, centrifugation and milling [1].

Population balance modeling is becoming more and more important in particulate processes since it provides a natural framework for the mathematical modeling of PSDs (e.g., see the tutorial article [2] and the review article [3]) and has been successfully applied to describe PSDs in many particulate processes. Population balance modeling of particulate processes typically leads to systems of nonlinear partial integro-differential equations that describe the rate of change of the PSD. The population balance models (PBMs) are also coupled with the material, momentum and energy balances that describe the rate of change of the state variables of the continuous phase, leading to complete particulate process models. As was pointed out by Christofides [4], the main difficulty in synthesizing practically implementable model-based, nonlinear feedback controllers for particulate processes is the distributed parameter nature of the PBMs, which does not allow their direct use for the synthesis of low-order (and therefore, practically imple-

* P. D. Christofides (corresponding author), J. Liu, Prof. J. F. Davis, Department of Chemical and Biomolecular Engineering, University of California, Los Angeles, CA 90095 (United States).
E-mail: pdc@seas.ucla.edu

** Prof. D. Muñoz de la Peña, Departmento de Ingeniería de Sistemas y Automática, Universidad de Sevilla, Camino de los Descubrimientos S/N, 41092, Sevilla (Spain).

mentable with available computers) nonlinear feedback controllers. To overcome this problem, earlier work of the current authors' group took advantage of the property that the dominant dynamic behavior of many particulate process models is low-dimensional and proposed [5] a model reduction procedure. This procedure is based on a combination of the method of weighted residuals and the concept of approximate inertial manifold and leads to the construction of low-order ordinary differential equation (ODE) systems that accurately reproduce the dominant dynamics of broad classes of particulate process models. These ODE systems were subsequently used for the synthesis of nonlinear [4–6], robust [7, 8] and predictive [9, 10] controllers that enforce desired stability, performance, robustness and constraint handling properties in the closed-loop system. In addition to these results, an online optimal control methodology including various performance objectives was developed for a seeded batch cooling crystallizer by Xie et al. [11] and Zhang and Rohani [12]. The reader may refer to other publications for reviews of results on simulation and control of particulate processes [13–16].

All of the above results on controller design for particulate processes are based on the assumption of continuous sampling and perfect communication between the sensor and the controller. However, one may encounter measurement sample loss, intermittent failures associated with measurement techniques, as well as data packet losses over communication networks. Previous work on control subject to actuator/sensor faults has primarily focused on lumped parameter systems. Specifically, El-Farra et al. [17], modeled communication losses as delays in implementing the control action, and reconfiguration-based strategies were devised to achieve fault-tolerance subject to faults in the control actuators by Mhaskar et al. [18]. In addition, Mhaskar et al. [19] also developed a theoretical framework for the modeling, analysis and reconfiguration-based fault-tolerant control of nonlinear processes subject to asynchronous sensor data losses, and the method was applied to a lumped parameter polyethylene reactor model. In addition, in a recent work by Gani et al. [20], a Lyapunov-based nonlinear controller was designed in the presence of input constraints to stabilize a continuous crystallizer subject to asynchronous sensor data losses. These works presume that a controller is designed under the assumption of continuous measurements, and the robustness properties of the closed-loop system under data losses or actuator/sensor faults are then studied.

Within control theory, most of the work on the subject of feedback control under asynchronous feedback or sampling has been performed in the context of networked control systems (NCS). NCS are control systems that have the control loops closed via a network and can often be modeled as asynchronous dynamical systems [21, 22]. The stability and disturbance attenuation issues for a class of linear NCS subject to data losses were modeled as a discrete-time switched linear system with arbitrary switching and were studied by Lin and Antsaklis [23]. Hassibi et al. [24] have studied the stability properties of a class of NCS modeled as linear asynchronous systems. NCS in which the plant is modeled by a nonlinear system have received less attention. Limited access systems where each unit must compete with the others for access to the network have also been studied within a sampled-data system framework [25, 26]. In these works, the practical stability of the system is guaranteed if the maximum time for which access to the network is not available is smaller than a given constant denoted as the maximum allowable transmission interval (MATI). Other recent results have dealt with the stability of continuous nonlinear systems under Lyapunov-based control subject to data losses [19]. A common theme of the above mentioned works is that the controller is designed without taking the network dynamics into account, and subsequently, the robustness of the closed-loop system in the presence of the network dynamics is studied. In another recent line of work, Montestruque and Antsaklis [27, 28] have proposed a strategy based on using an estimate of the state computed via the nominal model of the plant to decide the control input over the period of time in which feedback is lost between consecutively received measurements. This framework was applied to optimize the bandwidth needed by a networked control system modeled as a sampled-data linear system with variable sampling rate. Other relevant works related to this approach include those of Kim et al. [29, 30], where different control schemes were applied to a magnetic levitation test-bed controlled through a network. To the best of the current authors' knowledge, there are no previous results on the control of particulate processes with asynchronous measurements.

In the present work, nonlinear model predictive control is applied to a continuous crystallization process subject to asynchronous measurement sampling. Asynchronous measurement sampling may arise due to measurement system malfunctions or different sampling rates of the measurement sensors. In particular, a standard model predictive controller, a Lyapunov-based model predictive controller proposed by Mhaskar et al. [31, 32], and a Lyapunov-based model predictive controller developed in recent work by the current authors [33], which is designed taking into account explicitly data losses and asynchronous measurements, are applied to stabilize

the continuous crystallizer at an open-loop, unstable steady-state. Extensive simulations are presented to evaluate the closed-loop stability and robustness of the three control methods with three different assumptions on how the measurements from the crystallizer are obtained.

The paper is organized as follows: In section 2, the population balance model of a continuous crystallizer and the corresponding reduced-order moments model are introduced. In section 3, the modeling of a closed-loop system subject to asynchronous measurements is addressed. In section 4, three different model predictive controllers are introduced. In section 5, the simulations results are presented, while some concluding remarks are presented in section 6.

2 Model of a Continuous Crystallizer

In this section the population balance model of a continuous crystallizer and the corresponding reduced-order moments model are introduced.

2.1 Population Balance Model

Under the assumptions of isothermal operation, constant volume, mixed suspension, nucleation of crystals of infinitesimal size, and mixed product removal, a dynamic model for a continuous crystallizer can be derived from a population balance for the particle phase and a mass balance for the solute concentration. The resulting model has the following form [34, 35]:

$$\frac{\partial n}{\partial \bar{t}} = -\frac{\partial (R(\bar{t})n)}{\partial r} - \frac{n}{\tau} + \delta(r-0)Q(\bar{t})$$

$$\frac{dc}{d\bar{t}} = \frac{(c_0-\rho)}{\bar{\varepsilon}\tau} + \frac{(\rho-c)}{\tau} + \frac{(\rho-c)}{\bar{\varepsilon}}\frac{d\bar{\varepsilon}}{d\bar{t}}, \qquad (1)$$

where $n(r,\bar{t})$ is the number density of crystals of radius $r \in [0,\infty)$ at time $\bar{t}$ in the suspension, τ is the residence time, c is the solute concentration in the crystallizer, c_0 is the solute concentration in the feed, $\bar{\varepsilon} = 1 - \int_0^\infty n(r,\bar{t})\frac{4}{3}\pi r^3 dr$ is the volume of liquid per unit volume of suspension, $R(\bar{t})$ is the growth rate, $\delta(r-0)$ is the standard Dirac function, ρ is the density of crystals and $Q(\bar{t})$ is the nucleation rate. The term $\delta(r-0)Q(\bar{t})$ accounts for the production of crystals of infinitesimal (zero) size via nucleation. $R(\bar{t})$ and $Q(\bar{t})$ are assumed to follow McCabe's growth law and Volmer's nucleation law, respectively, i.e.:

$$R(\bar{t}) = k_1(c-c_s),\ Q(\bar{t}) = \bar{\varepsilon}k_2 \exp\left[-k_3/\left(c/c_s-1\right)^2\right], \qquad (2)$$

where k_1, k_2, and k_3 are positive constants and c_s is the concentration of the solute at saturation.

The values of the parameters in Eqs. (1) and (2) that define the process studied in this work are given in Table 1. The open-loop crystallizer model exhibits a highly oscillatory behavior, which is the result of the interplay between growth and nucleation caused by the relative nonlinearity of the nucleation rate as compared to the growth rate. A detailed discussion on the nature of the oscillations exhibited by this process is given elsewhere [5]. The population model introduced provides a good approximation of the dynamics of a continuous crystallizer [4]. All simulations have been carried out using the model given by Eq. (1).

Table 1: Process parameters of the continuous crystallizer.

c_s	=	980.2	$kg\ m^{-3}$
c_{0s}	=	999.943	$kg\ m^{-3}$
ρ	=	1770.0	$kg\ m^{-3}$
τ	=	1.0	hr
k_1	=	5.065×10^{-2}	$mm\ m^3\ kg^{-1}\ hr^{-1}$
k_2	=	7.958	$mm^{-3}\ hr^{-1}$
k_3	=	1.217×10^{-3}	

2.2 Reduced-Order Moments Model

The population balance model is not appropriate for synthesizing model-based, low-order feedback control laws due to its distributed parameter nature. To overcome this problem, following the same approach as previously presented by the current authors [5], a reduced-order moments model, which accurately reproduces the dominant dynamics of the system and is suitable for directly synthesizing low-order feedback control laws, is deduced.

The j th moment of $n(r,\bar{t})$ is defined by:

$$\mu_j = \int_0^\infty r^j n(r,\bar{t})dr,\ \ j = 0,1,...,\infty. \qquad (3)$$

By multiplying the population balance in Eq. (1) by r^j, integrating over all particle sizes, and introducing the following set of dimensionless variables and parameters:

$$\tilde{x}_0 = 8\pi\sigma^3\mu_0,\ \tilde{x}_1 = 8\pi\sigma^2\mu_1,\ \tilde{x}_2 = 4\pi\sigma\mu_2,\ \tilde{x}_3 = \frac{4}{3}\pi\mu_3, ...,$$

$$t = \frac{\bar{t}}{\tau},\ \sigma = k_1\tau(c_{0s} - c_s),\ Da = 8\pi\sigma^3 k_2\tau,$$

$$F = \frac{k_3 c_s^2}{(c_{0s} - c_s)^2}, a = \frac{(\rho - c_s)}{(c_{0s} - c_s)}, \tilde{y} = \frac{(c - c_s)}{(c_{0s} - c_s)}, u = \frac{(c_0 - c_{0s})}{(c_{0s} - c_s)}, \tag{4}$$

where c_{0s} is the steady-state solute concentration in the feed, the dominant dynamics of Eq. (1) can be adequately captured by the following fifth-order moments model, which includes the dynamics of the first four moments and those of the solute concentration:

$$\frac{d\tilde{x}_0}{dt} = -\tilde{x}_0 + (1 - \tilde{x}_3) Da e^{\frac{-F}{\tilde{y}^2}}$$

$$\frac{d\tilde{x}_1}{dt} = -\tilde{x}_1 + \tilde{y}\tilde{x}_0$$

$$\frac{d\tilde{x}_2}{dt} = -\tilde{x}_2 + \tilde{y}\tilde{x}_1$$

$$\frac{d\tilde{x}_3}{dt} = -\tilde{x}_3 + \tilde{y}\tilde{x}_2$$

$$\frac{d\tilde{y}}{dt} = \frac{1 - \tilde{y} - (a - \tilde{y})\tilde{y}\tilde{x}_2}{1 - \tilde{x}_3} + \frac{u}{1 - \tilde{x}_3}, \tag{5}$$

where $\tilde{x}_v$, $v = 0, 1, 2, 3$ are dimensionless moments of the crystal size distribution, $\tilde{y}$ is the dimensionless concentration of the solute in the crystallizer and u is a dimensionless concentration of the solute in the feed. The values of the dimensionless model parameters in Eq. (4) are given in Table 2. It should be noted that since the moments of order four and higher do not affect those of order three and lower, the state of the infinite dimensional system is bounded when $\tilde{x}_3$ and $\tilde{y}$ are bounded, and it converges to a globally exponentially stable equilibrium point when $\lim_{t\to\infty} \tilde{x}_3 = c_1$ and $\lim_{t\to\infty} \tilde{y} = c_2$, where c_1, c_2 are constants. In this work, the state of the crystallizer is denoted as $\tilde{x} = [\tilde{x}_0\ \tilde{x}_1\ \tilde{x}_2\ \tilde{x}_3\ \tilde{y}]^T$, and the reduced-order moments model is used to define different model predictive control strategies.

Table 2: Dimensionless parameters of the continuous crystallizer.

σ	=	$k_1\tau(c_{0s} - c_s)$	=	$1.0\,mm$
Da	=	$8\pi\sigma^3 k_2\tau$	=	200.0
F	=	$k_3 c_s^2/(c_{0s} - c_s)^2$	=	3.0
a	=	$(\rho - c_s)/(c_{0s} - c_s)$	=	40.0

The reduced-order moments model is a very good approximation of the population balance model and is suitable for directly synthesizing model-based, low-order, feedback control laws. The reader may refer to previous work by the current authors [5, 8] for a detailed derivation of the moments model, and for further results and references in this area [4]. The stability properties of the fifth-order model of Eq. (5) have been also studied, and it has been shown [35] that the global phase space of this model has a unique unstable steady-state surrounded by a stable periodic orbit at:

$$\tilde{x}_s = [\tilde{x}_{0s}\ \tilde{x}_{1s}\ \tilde{x}_{2s}\ \tilde{x}_{3s}\ \tilde{y}_s]^T$$

$$= [0.0471\ 0.0283\ 0.0169\ 0.0102\ 0.5996]^T,$$

and that the linearization of Eq. (1) around the unstable steady-state includes two isolated complex conjugate eigenvalues with a positive real part. The control objective is to regulate the system to the unstable steady-state, $\tilde{x}_s$, by manipulating the solute feed concentration c_0.

Constraints have to be considered in the input. The dimensionless solute feed concentration, u, is subject to the constraints: $-u_{max} \le u \le u_{max}$, where $u_{max} = 3$. For $u_{max} = 3$, the constraint on the inlet solute concentration corresponds to $940\ kg/m^3 \le c_0 \le 1060\ kg/m^3$.

The state x is denoted as the error, i.e., $x = \tilde{x} - \tilde{x}_s$. Then, one can rewrite Eq. (5) in a more compact form as follows:

$$\dot{x}(t) \quad = \quad f(x(t)) + g(x(t))u(t), \tag{6}$$

where $x = [x_0\ x_1\ x_2\ x_3\ y]^T$, and f and g have the following form:

$$f(x) = \begin{bmatrix} -(x_0 + \tilde{x}_{0s}) + (1 - x_3 - \tilde{x}_{3s}) Da e^{\frac{-F}{(\tilde{y}+\tilde{y}_s)^2}} \\ -(x_1 + \tilde{x}_{1s}) + (y + \tilde{y}_s)(x_0 + \tilde{x}_{0s}) \\ -(x_2 + \tilde{x}_{2s}) + (y + \tilde{y}_s)(x_1 + \tilde{x}_{1s}) \\ -(x_3 + \tilde{x}_{3s}) + (y + \tilde{y}_s)(x_2 + \tilde{x}_{2s}) \\ \frac{1 - y - \tilde{y}_s - (a - y - \tilde{y}_s)(y + \tilde{y}_s)(x_2 + \tilde{x}_{2s})}{1 - x_3 - \tilde{x}_{3s}} \end{bmatrix},$$

$$g(x) = \begin{bmatrix} 0 \\ 0 \\ 0 \\ 0 \\ \frac{1}{1 - x_3 - \tilde{x}_{3s}} \end{bmatrix}$$

At this stage, a feedback control law is defined as $h_L : R^n \rightarrow R$, which satisfies $h_L(0) = 0$ and renders the origin $x = 0$ of the closed-loop system of Eq. (6) asymptotically stable under continuous measurements. Stabilizing state feedback control laws for nonlinear systems have been developed using Lyapunov techniques and result in this are presented elsewhere [36, 37]. In this work, the Lyapunov-based feedback control proposed by Lin and Sontag [38] is used (see also [39, 40]), which is based on a control Lyapunov function of the open-loop system.

Consider the control Lyapunov function $V(x) = x^T Px$ with $P = I$ of the system of Eq. (6). The following Lyapunov-based feedback control law asymptotically stabilizes the open-loop unstable steady-state under continuous state feedback implementation for an appropriate set of initial conditions [38]:

$$h_L(x) = -k(x)L_gV(x), \tag{7}$$

where

$$k(x) = \begin{cases} \dfrac{L_fV(x) + \sqrt{\left(L_fV(x)\right)^2 + \left(u_{max}L_gV(x)\right)^4}}{\left(L_gV(x)\right)^2\left[1 + \sqrt{1 + \left(u_{max}L_gV(x)\right)^2}\right]}, & L_gV(x) \neq 0 \\ 0, & L_gV(x) = 0. \end{cases}$$

with $L_fV(x) = \frac{\partial V(x)}{\partial x}f(x)$ and $L_gV(x) = \frac{\partial V(x)}{\partial x}g(x)$. The feedback controller, $h_L(x)$, will be used to design the contractive constraints of the two Lyapunov-based model predictive controllers, which are presented in section 4.

3 Modeling Asynchronous Measurements

Most control systems assume that the measurements from the sensors are obtained in a continuous periodic pattern and that the communications between the different components of the system are flawless. However, these assumptions do not hold in many processes due to a host of measurement difficulties and possible errors in communications, e.g., if wireless links are used to implement the control system. In this case, the system is subject to asynchronous measurements. Measuring the concentration and the properties of the PSD of a continuous crystallizer is a difficult task that might take variable lengths of time. It is assumed that the sampling of the state of the continuous crystallizer of Eq. (1) takes at least 15 min, and if errors occur in the sampling system or in the communication network, it may take a much longer time. It is also assumed that the maximum time interval (worst case occurrence) between two consecutive measurements is shorter than 2.5 h, which is denoted as T_{max}. Note that a T_{max} value is needed in the present stabilization problem because the open-loop crystallizer is unstable.

Simulation results under three different assumptions on how the measurements from the crystallizer are obtained will be presented in section 5. In this section, the method for modeling sampled-data systems subject to asynchronous measurements, is presented. To account for asynchronous sampling, the sampling times are defined by an increasing time sequence, $\{t_{k\geq 0}\}$. At each sampling time, t_k, a new measurement is obtained from the sensors. The interval between two consecutive samplings is not fixed. In the simulation section, three different ways of generating the time sequence $\{t_{k\geq 0}\}$ are presented. The only assumption made on the time sequence $\{t_{k\geq 0}\}$ is that there is an upper bound on the maximum time in which the system operates in open-loop, i.e., T_{max}. This bound on the maximum period of time in which the loop is open has been also used in other studies [19, 25, 27] and is required in the present stabilization problem since the open-loop crystallizer is unstable.

This paper also accounts for the fact that the controller may not receive the whole state (x_0, x_1, x_2, x_3, y) at each sampling instant, i.e., the state of PSD, (x_0, x_1, x_2, x_3) or the solute concentration, y (see Figures 1 and 2) may be transmitted only at a specific time instant. This is due to the fact that PSD and solute concentration are measured by different sensors with different sampling rates. At a sampling time t_k, if only part of the state is available, an estimation of the current state $\hat{x}(t_k)$ is obtained and sent to the controller to generate a new control input. An auxiliary variable $s(t_k)$ is used to indicate the part of the process state that is available at sampling time t_k as follows:

1) $s(t_k) = 1$ implies that both measurements of PSD and solute concentration are available at t_k, and $\hat{x}(t_k) = x(t_k)$.
2) $s(t_k) = 2$ implies that only the measurement of PSD is available at t_k. The corresponding value of the

solute concentration at t_k is estimated by using the last available value of solute concentration, i.e., $\hat{y}(t_k) = \hat{y}(t_{k-1})$.

3) $s(t_k) = 3$ implies that only the measurement of solute concentration is available at t_k. The corresponding state of PSD at t_k is estimated by the reduced-order moments model of Eq. (6). The last available estimated state $\hat{x}(t_{k-1})$ is taken as the initial state.

The estimated state used by the controller at each sampling time is given by the following expression:

$$\hat{x}(t_k) = \begin{cases} x(t_k) & \text{if } s(t_k) = 1 \\ \{x_0(t_k), x_1(t_k), x_2(t_k), x_3(t_k), \hat{y}(t_{k-1})\} & \text{if } s(t_k) = 2 \\ \{\hat{x}_0(t_k), \hat{x}_1(t_k), \hat{x}_2(t_k), \hat{x}_3(t_k), y(t_k)\} & \text{if } s(t_k) = 3, \end{cases} \tag{8}$$

where $\hat{x}_v, v = 0, 1, 2, 3$, are estimated by using the reduced-order moments model. It should be noted that one has to store the implemented manipulated input trajectory.

Remark 1. *Note that regardless of the method used to estimate the state when only partial state information is available, errors exist between the estimated state $\hat{x}$ and the actual state of the system x, that have to be compensated by the available feedback.*

In this class of processes, the solute concentration is obtained with a higher sampling rate than the crystallizer PSD. This motivates the use of the last available value of the solute concentration when a new PSD measurement is obtained. On the other hand, instead of using the last available values of the PSD each time a new concentration measurement is undertaken, which may introduce a large error because the PSD is sampled less frequently, the reduced-order moments model can be used to estimate the missing information, which increases the computational complexity but decreases the estimation error.

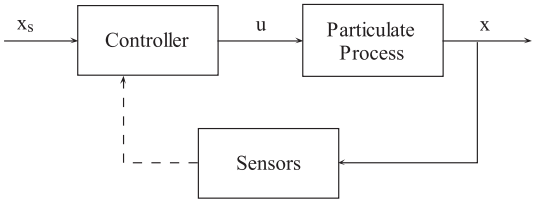

Fig. 1: Closed-loop system with asynchronous measurements. The entire state is sampled at the same time instants.

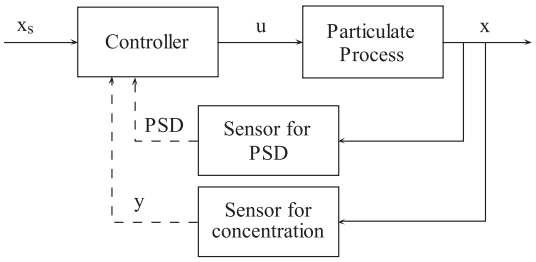

Fig. 2: Closed-loop system with asynchronous measurements. The states of the PSD and solute concentration are sampled asynchronously.

The controller has to take into account that the measurements arrive in an asynchronous manner and that the time in which it has to operate in open-loop may be lengthy. In order to decide the manipulated input $u(t)$, that has to be applied at each time t, the controller uses the last estimated state $\hat{x}(t_k)$ and the corresponding sampling time t_k. It is assumed that each controller is defined by a function $h(\Delta, \hat{x}(t_k))$, where $\hat{x}$ is the last available estimated state and Δ is the time that has passed since that state was received. This function allows one to model different implementation strategies, e.g., $h(\Delta, \hat{x}) = h_L(\hat{x})$ implements a sample-and-hold strategy based on the Lyapunov-based controller of Eq. (7). In this case, the input is maintained constant between samples independently of the time Δ that has passed since the last measurement.

In order to consider the models in this work in a unified time scale and with the same manipulated input, Eq. (2), the expressions of dimensionless time, t, and manipulated input, u, are all substituted into Eq. (1). Therefore, the following asynchronous nonlinear model for the closed-loop system of the crystallizer is obtained:

$$\begin{aligned} \frac{1}{\tau}\frac{\partial n}{\partial t} &= -k_1(c - c_s)\frac{\partial n}{\partial r} - \frac{n}{\tau} + \delta(r - 0)\bar{\varepsilon}k_2 exp \\ &\quad \left[-k_3/\left(c/c_s - 1\right)^2\right] \\ \frac{1}{\tau}\frac{dc}{dt} &= \frac{(c_{0s} - \rho)}{\bar{\varepsilon}\tau} + \frac{(\rho - c)}{\tau} + \frac{(\rho - c)}{\bar{\varepsilon}\tau}\frac{d\bar{\varepsilon}}{dt} + \frac{(c_{0s} - c_s)u(t)}{\bar{\varepsilon}\tau}, \\ & \quad t \in [t_k, t_{k+1}] \\ u(t) &= h(t - t_k, \hat{x}(t_k)). \end{aligned} \tag{9}$$

At time t_k, new information is available from the sensors and the content of the information is decided by the corresponding value of $s(t_k)$. The state $\hat{x}(t_k)$ is an estimation of the actual state $x(t_k)$ and it is estimated by the approach presented earlier in this section, see Eq. (8). The controller generates a future manipulated input trajectory $h(\Delta, \hat{x})$ that depends on this estimated state, where Δ is the time that has passed since t_k.

4 Model Predictive Control

Model predictive control (MPC) is a popular control strategy based on using a model of the process to predict, at each sampling time, the future evolution of the system from the current state along a given prediction horizon. Using these predictions, the manipulated input trajectory that minimizes a given performance index is computed by solving a suitable optimization problem. To obtain finite-dimensional optimization problems, MPC optimizes the system over the family of piecewise constant trajectories with a fixed sampling time and a fixed prediction horizon, i.e., a fixed length. This implies that the MPC controllers are implemented in a sample and hold scheme. The MPC framework is particularly appropriate for controlling systems subject to asynchronous measurements because the actuator can profit from the predicted evolution of the system, to update the manipulated input when feedback is lost, instead of setting the manipulated input to a fixed value, which is usually zero or to the last implemented manipulated input. In this section, three different MPC controllers, i.e., a standard model predictive controller and two recently proposed Lyapunov-based model predictive controllers are introduced. These controllers are based on the reduced-order moments model of Eq. (6) and the Lyapunov-based controller of Eq. (7) presented in section 2.

4.1 Standard Model Predictive Control

The standard MPC controller used in this paper is based on the following optimization problem [41]:

$$\begin{aligned} J^*(\hat{x}) = \min_{u(\tau)\in S(\Delta_c)} \quad & \int_0^{N\Delta_c} [x(\tau)^T Q_c x(\tau) + u(\tau)^T R_c u(\tau)] d\tau \\ \text{s.t.} \quad & \dot{x}(\tau) = f(x(\tau)) + g(x(\tau))u(\tau) \\ & x(0) = \hat{x} \\ & |u(\tau)| \le u_{max}, \ \forall \tau \in [0, N\Delta_c], \end{aligned} \tag{10}$$

where $S(\Delta_c)$ is the family of piece-wise constant functions with a sampling period Δ_c, $x(\tau)$ is the predicted trajectory of the system by the reduced-order moments model for the manipulated input trajectory computed by the MPC, Q_c, R_c are positive definite weight matrices that define the cost, $\hat{x}$ is the initial condition, and u_{max} is the bound on the control action.

The initial state is provided as a parameter to the MPC optimization problem. For a given time step, a new estimate of the actual state, $\hat{x}$, is obtained, the optimization problem defined in Eq. (10) is solved to obtain the optimal manipulated input trajectory, $u^*(\tau)$, of length $N\Delta_c$. Usually, only the first move of the trajectory ($u(\tau) \in [0, \Delta_c]$) is used. This is the standard receding horizon strategy and it does not take into account that the state might not be available at a given sampling time due to data losses or asynchronous measurement sampling. The control law corresponding to the MPC controller that takes into account asynchronous measurements is defined as follows:

$$h(\Delta, \hat{x}) = u^*(\Delta),$$

where u^* is the solution of the optimization problem defined in Eq. (10) for an initial state $x(0) = \hat{x}$. It should be noted that this control law is not defined for all times. The optimal trajectory, u^*, is of length $N\Delta_c$. This limits the maximum time in which the MPC controller can operate in the open-loop configuration.

It should also be noted that the MPC of Eq. (10) assumes a given sampling time, Δ_c, which is independent of the asynchronous sampling sequence that defines the closed-loop system as discussed in section 3, i.e., the MPC scheme defines a sampling time to describe the optimization problem and is different from the actual sampling time of the process.

4.2 Lyapunov-based Model Predictive Control I

The standard MPC controller used in this work is based on minimizing a given cost function defined by matrices Q_c and R_c, using the reduced-order moments model subject to constraints on the input. No additional constraints are used to guarantee closed-loop stability properties. In order to guarantee the stability and robustness of the closed-loop system, the MPC optimization problem has to be modified. In this subsection, the Lyapunov-based model predictive controller (LMPC) proposed by Mhaskar et al. [31,32] is presented. This controller guarantees the practical stability of the closed-loop system under the assumption of synchronous measurements and no measurement unavailability. The controller is based on the previously designed Lyapunov-based controller, h_L, that guarantees asymptotic stability of the closed-loop system under continuous measurements. It is used to define a contractive constraint, which guarantees that the LMPC inherits the stability and robustness properties of the Lyapunov-based controller. The controller introduced by Mhaskar et al. [31,32] is based on the following optimization problem:

$$J^*(\hat{x}) = \min_{u(\tau)\in S(\Delta_c)} \int_0^{N\Delta_c} [x(\tau)^T Q_c x(\tau) + u(\tau)^T R_c u(\tau)] d\tau \quad (11a)$$

$$\text{s.t. } \dot{x}(\tau) = f(x(\tau)) + g(x(\tau))u(\tau) \quad (11b)$$

$$x(0) = \hat{x} \quad (11c)$$

$$|u(\tau)| \leq u_{max},\ \forall\ \tau\in[0,\ N\Delta_c] \quad (11d)$$

$$\frac{\partial V(\hat{x})}{\partial \hat{x}} f(\hat{x}, u(0)) \leq \frac{\partial V(\hat{x})}{\partial \hat{x}} f(\hat{x}, h_L(\hat{x})). \quad (11e)$$

The constraint of Eq. (11e) guarantees that the value of the time derivative of the control Lyapunov function at the initial evaluation time of the LMPC is lower or equal to the value obtained when the value of the Lyapunov-based controller $u = h_L(x)$ is implemented in the closed-loop system. This is the contractive constraint that allows one to prove (when no measurement unavailability is taken into account) that the LMPC inherits the stability and robustness properties of the Lyapunov-based controller, h_L. The corresponding function, $h(\Delta, \hat{x})$, is defined as in the standard MPC case.

4.3 Lyapunov-based Model Predictive Control II

In this section, the Lyapunov-based model predictive control law developed by Muñoz de la Peña and Christofides [33] is given. This control law takes into account data losses and asynchronous measurements explicitly. In order to present the optimization problem that defines this LMPC, one needs the following definition:

Definition 1. *The sampled trajectory of Eq. (6) of length $N\Delta_c$ associated with the Lyapunov-based feedback control law, $h_L(x)$, with initial state, $x_L(0)$, is denoted by $x_L(\tau)$ and is obtained by solving Eq. (12) recursively:*

$$\begin{aligned} \dot{x}_L(\tau) &= f(x_L(\tau)) + g(x_L(\tau))u(\tau_k),\ \tau\in[\tau_k, \tau_{k+1}] \\ u(\tau_k) &= h_L(x_L(\tau_k)) \end{aligned} \quad , \quad (12)$$

where $\tau_k = k\Delta_c$ and $k = 0, ..., N-1$.

The sampled trajectory of Eq. (6) associated with the Lyapunov-based feedback control law, $h_L(x)$, is the state trajectory of the crystallizer in closed-loop with the Lyapunov-based controller applied in a sample-and-hold scheme. This state trajectory is used to define the contractive constraint of the following LMPC optimization problem:

$$J^*(\hat{x}) = \min_{u(\tau)\in S(\Delta_c)} \int_0^{N\Delta_c} [x(\tau)^T Q_c x(\tau) + u(\tau)^T R_c u(\tau)] d\tau \quad (13a)$$

$$\text{s.t. } \dot{x}(\tau) = f(x(\tau)) + g(x(\tau))u(\tau) \quad (13b)$$

$$x(0) = \hat{x} \quad (13c)$$

$$|u(\tau)| \leq u_{max},\ \forall\ \tau\in[0,\ N\Delta_c] \quad (13d)$$

$$V(x(\tau)) \leq V(x_L(\tau)),\ \forall\ \tau\in[0,\ N\Delta_c], \quad (13e)$$

where $x_L(\tau)$ is the sampled trajectory of Eq. (6) of definition 1 for an initial state $x_L(0) = \hat{x}$.

The main difference between the LMPC of Eq. (13) and the LMPC of Eq. (11) presented in the last subsection is the contractive constraint. The constraint of Eq. (11e) guarantees that the LMPC controller of Eq. (11) provides at least the same decrease of the control Lyapunov function as the Lyapunov-based controller in the first time step. When data losses or asynchronous measurements are taken into account, in order to prove that the LMPC of Eq. (13) inherits the same properties of the Lyapunov-based controller, the contractive constraint of Eq. (13e) must hold along the entire prediction horizon. In this manner, when measurements are unavailable, the optimal manipulated input trajectory evaluated guarantees that the predicted decrease of the control Lyapunov function is at least equal to the one obtained by applying the Lyapunov-based controller. The corresponding function $h(\Delta, \hat{x})$ is defined as in the MPC case.

Remark 2. *The contractive constraints of Eqs. (11e) and (13e) are needed to ensure stability of the closed-loop moments model, and therefore, of the full infinite-dimensional closed-loop system, under the LMPC of Eqs. (11) and (13) in the presence of synchronous and asynchronous sampling, respectively. Without these contractive constraints, the stability of the closed-loop system cannot be guaranteed. However, the addition of these contractive constraints facilitates the proof of the feasibility of the LMPC and closed-loop stability for a well-characterized set of initial conditions [31, 32, 33] for the lumped parameter moments model.*

Remark 3. S*ystems subject to bounded uncertainties have been studies elsewhere [31, 32, 33] and it was shown that if the LMPC controllers are appropriately designed, they guarantee a certain degree of stability and robustness properties of the closed-loop system that depend on the size of the set that bounds the uncertainty. If the estimation errors are bounded (as in this particular case), they can be included as part of the uncertainty of the system, increasing in some way the effect of the uncertainty and*

the set in which they are bounded. This implies that all the LMPC controllers used in this work possess a certain robustness property with respect to modeling and estimation errors (see also the numerical results in the next section).

It should be noted that the three model predictive controllers presented in this section assume the same sampling time Δ_c. In most control systems where the measurements are obtained synchronously and the communications are flawless, this sampling time is equal to the sampling time used to obtain new measurements and implement the manipulated input (sample-and-hold schemes). However, this study deals with systems subject to asynchronous measurements, and the time sequence as discussed in section 3 that determines when new information is available, is independent of Δ_c.

4.4 MPC Parameters

In the remainder of this work, the three model predictive controllers of Eqs. (10–13) are denoted as MPC, LMPC I and LMPC II, respectively. The cost functions of these controllers are defined by matrices $Q_c = P$ and $R_c = 4$. The weight matrices Q_c and R_c have been chosen to provide a performance similar to the one of the Lyapunov-based controllers under a sample-and-hold implementation. The sampling time of the MPC controllers is $\Delta_c = 0.25$ h, which is equal to the minimum time needed to obtain a new measurement.

Through simulations, the transition time for the crystallizer in closed-loop with the Lyapunov-based controller has been estimated as 2 h for states x_0, y and 4 h for states x_1, x_2, x_3. The prediction horizon $N = 11$ is chosen for the model predictive controllers so that the prediction captures most of the dynamic evolution of the process.

5 Simulation Results

In this section, the three model predictive control laws MPC, LMPC I and LMPC II are applied to the continuous crystallizer population balance model of Eq. (9) to evaluate the stability and robustness properties of the corresponding closed-loop systems in the presence of measurement unavailability and asynchronous measurements. Firstly, PSD and solute concentration sampled synchronously and simultaneously subject to measurement unavailability are simulated. Following that, the system with asynchronous measurements in which measurements of PSD and solute concentration are obtained simultaneously are simulated, followed by simulation of the system with asynchronous measurements in which PSD and solute concentration are sampled at different time instants. The control objective is to suppress the oscillatory behavior of the crystallizer and stabilize it at the open-loop unstable steady-state, $\tilde{x}_s$, that corresponds to the desired PSD by manipulating the solute feed concentration. The following initial conditions are used in the simulations:

$$n(0,r) = 0.0,\ c(0) = 990.0\ kg\ m^{-3},\ \tilde{x}(0) = [0\ 0\ 0\ 0\ 0.498]^T. \tag{14}$$

A second-order accurate finite-difference discretization scheme is used to simulate the continuous crystallizer. At every model evaluation step (which is different from the sampling time and should be chosen to be sufficiently small in order to get a continuous and accurate solution) of Eq. (9), the values of $n(t,r)$ and $c(t)$ can be obtained, so that they can be used to calculate the state x at that time using Eqs. (3) and (4) and the steady-state $\tilde{x}_s$.

5.1 Results of Synchronous Sampling Subject to Measurement Unavailability

For this set of simulations, it is assumed that a new measurement of the whole state of the crystallizer is made every Δ_m, the synchronous sampling time, but that the measurement might be lost due to errors in the measurement or communication systems with a probability $p \in (0,1)$. To generate the time partition $\{t_{k\geq 0}\}$ that indicates when a new sample is available and the corresponding auxiliary variable $s(t_k)$ for a simulation of length t_{sim}, the following algorithm is used:

$t_0 = 0, k = 0$

while $t_k < t_{sim}$

  $t_{k+1} = t_k, \gamma = 0$

  while $\gamma \leq p$

  end $t_{k+1} = t_{k+1} + \Delta_m, \gamma = rand\,(1)$

  if $t_{k+1} > t_k + T_{max}$ then $t_{k+1} = t_k + T_{max}$

  $s(t_k) = 1, k = k + 1$

end

where t_{sim} is the simulation time, $rand(1)$ generates a uniformly distributed random value γ between 0 and 1, and T_{max} is the maximum allowable transmission interval.

As mentioned before T_{max} is taken to be 2.5 h, and the simulation time t_{sim} is 30 h in this work. The sampling

time Δ_m is equal to Δ_c, i.e., $\Delta_m = 0.25$ h. For this sampling time, the sampled-data system in a closed-loop with $u = h_L(x)$ is practically stable and its performance is similar to the closed-loop system with continuous measurements. A value of $\gamma = 95\,\%$ is chosen, i.e., there is a probability of 95 % that the measurement of the state is unavailable at every sampling time. Firstly, LMPC II is compared with MPC. The state and manipulated input trajectories of this simulation are shown in Figure 3. In this figure it can be seen that LMPC II provides a better performance than MPC. In particular, LMPC II is able to stabilize the process at the open-loop unstable steady-state in about 5 h while the system in closed-loop with MPC presents an oscillatory behavior indicating that the stabilization of the operating unstable steady-state has not been achieved. Secondly, LMPC II is compared with LMPC I. The state and manipulated input trajectories of this simulation are shown in Figure 4. In this case LMPC I is not able to regulate the system to the desired equilibrium. Finally, the two LMPC II controllers are compared using the predicted manipulated input trajectory and the "last implemented manipulated input", respectively. The "last implemented manipulated input" strategy keeps the manipulated input constant, i.e., $h(\Delta, \tilde{x}) = u^*(0)$ for all Δ where $u^*(\cdot)$ is the optimal solution of the optimization problem of Eq. (13) (the optimization problem that defines LMPC II) with an initial state $\tilde{x}$. The state and manipulated input trajectories of this simulation are shown in Figure 5. In this case, this simulation demonstrates that it is not possible

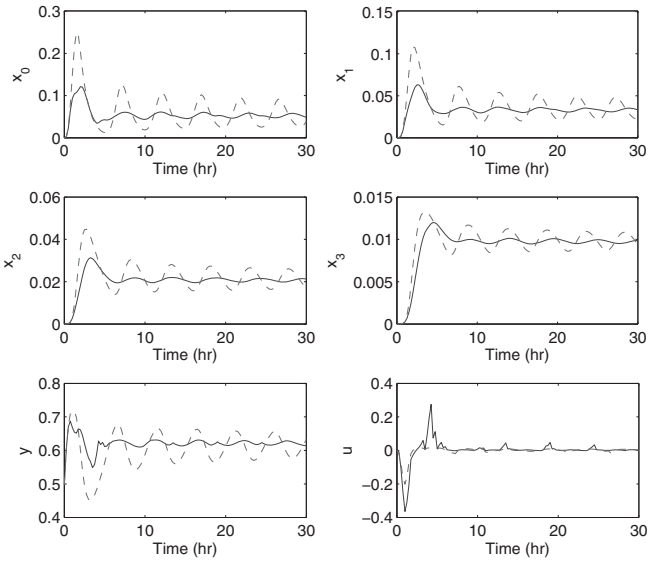

Fig. 3: State and manipulated input trajectories of Eq. (9) with PSD and solute concentration sampled synchronously and simultaneously, and 95 % probability of measurement unavailability using the predicted manipulated input trajectories of LMPC II of Eq. (13) (solid curves) and MPC of Eq. (10) (dashed curves).

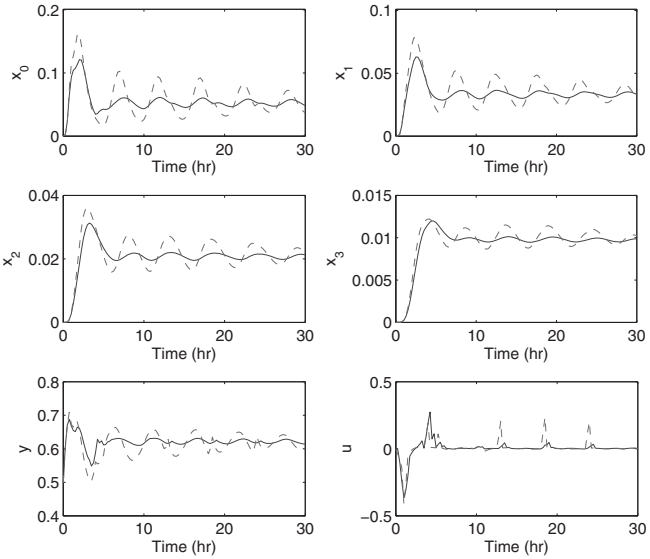

Fig. 4: State and manipulated input trajectories of Eq. (9) with PSD and solute concentration sampled synchronously and simultaneously, and 95 % probability of measurement unavailability using the predicted manipulated input trajectories of LMPC II of Eq. (13) (solid curves) and LMPC I of Eq. (11) (dashed curves).

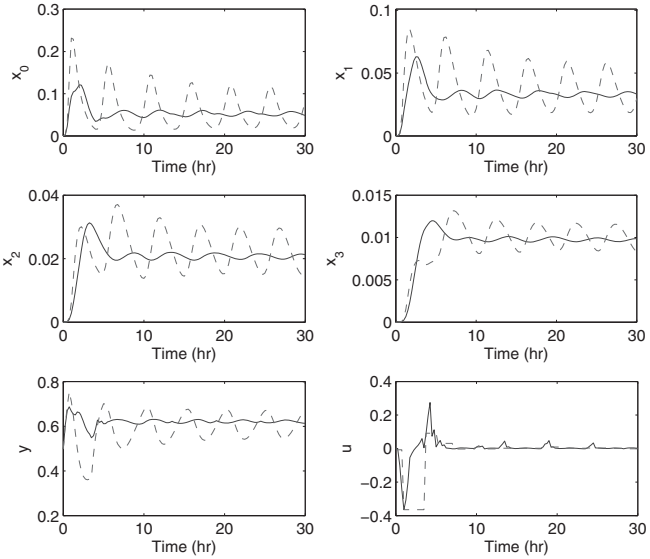

Fig. 5: State and manipulated input trajectories of Eq. (9) with PSD and solute concentration sampled synchronously and simultaneously, and 95 % probability of measurement unavailability using the predicted manipulated input trajectory (solid curves) and the last implemented manipulated input (dashed curves) of LMPC II of Eq. (13).

to maintain the process at the desired steady-state, using only the last implemented manipulated input.

The simulations demonstrate that LMPC II is more robust to measurements unavailability than MPC and LMPC I. This is because LMPC II is designed by explicitly taking measurement unavailability into account.

Moreover, one should make full use of the predicted manipulated input trajectory of LMPC II in order to get the best closed-loop system performance.

5.2 Results of Asynchronous Sampling: PSD and Solute Concentration Sampled Simultaneously

For the simulations in this subsection, it is assumed that the time between consecutive measurements is obtained using a random process and that the PSD and solute concentration are measured simultaneously. To generate the time intervals between samples, a random Poisson process is used, as described elsewhere [18, 20]. The Poisson process is defined by the number of events per unit time W. At a given time t, an event takes place which means that the state is sampled. The interval between two consecutive sampling times is given by $\Delta_a = \frac{-ln\chi}{W}$, where χ is a random variable with uniform probability distribution between 0 and 1. At $t + \Delta_a$, another event occurs. The sequence $\{t_{k\geq 0}\}$ and the corresponding auxiliary variable $s(t_k)$ for a simulation of length t_{sim} are generated as follows:

$t_0 = 0, k = 0$

while $t_k < t_{sim}$

$\chi = rand(1)$

$t_{k+1} = t_k + \frac{-ln\chi}{W}$

if $t_{k+1} > t_k + T_{max}$, then $t_{k+1} = t_k + T_{max}$

if $t_{k+1} < t_k + T_{min}$, then $t_{k+1} = t_k + T_{min}$

$s(t_k) = 1, k = k + 1$

end

where $rand(1)$ generates a uniformly distributed random value χ between 0 and 1, T_{max} is the maximum allowable transmission interval and T_{min} is the minimum time interval between two consecutive samplings. Note that T_{min} should be smaller than T_{max}, i.e., $T_{min} < T_{max}$. As mentioned before T_{max} is 2.5 h. The minimum time limit T_{min} is equal to the synchronous sampling time, i.e., $T_{min} = \Delta_m = 0.25$ h. For the simulations carried out in this subsection, the value of the number of events per unit time is chosen to be $W = 0.15$. The sampling times for the simulations are shown in Figure 6. Note that because the number of events is low, the time between consecutive samplings, and hence, the time in which the control system must operate in open-loop, may be large but will always be smaller than T_{max}.

The same comparisons are carried out as performed in section 5.1. Firstly, LMPC II is compared with MPC.

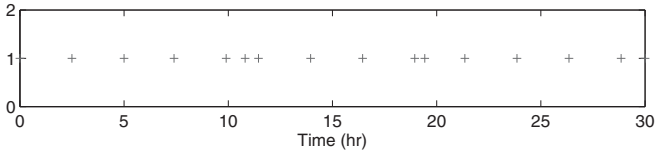

Fig. 6: Asynchronous sampling times for both, PSD and solute concentration.

The state and manipulated input trajectories of this simulation are shown in Figure 7. In this simulation, MPC cannot stabilize the process, while LMPC II is able to maintain the process at the desired steady-state. Secondly, LMPC II is compared with LMPC I. The state and manipulated input trajectories are shown in Figure 8. Though LMPC II and LMPC I can both stabilize the process, the transient of the closed-loop system under LMPC II is shorter than the transient under LMPC I and has a smaller overshoot. Finally, two LMPC II controllers are implemented using the predicted manipulated input trajectory and the last implemented manipulated input, respectively. As in the simulation of section 5.1, the last implemented manipulated input strategy is not able to stabilize the process.

From the results of this subsection, one can also conclude that LMPC II using the predicted manipulated input trajectory is the most robust in the presence of asynchronous sampling among the three controllers.

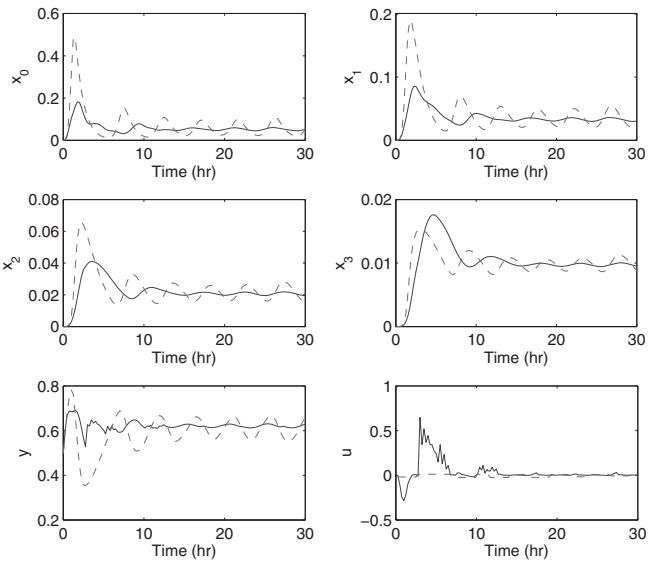

Fig. 7: State and manipulated input trajectories of Eq. (9) with PSD and solute concentration sampled asynchronously and simultaneously using the predicted manipulated input trajectories of LMPC II of Eq. (13) (solid curves) and MPC of Eq. (10) (dashed curves).

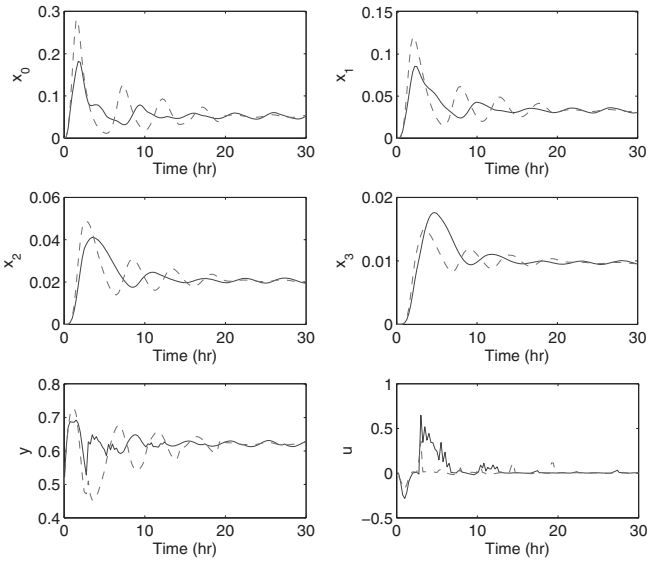

Fig. 8: State and manipulated input trajectories of Eq. (9) with PSD and solute concentration sampled asynchronously and simultaneously using the predicted manipulated input trajectories of LMPC II of Eq. (13) (solid curves) and LMPC I of Eq. (11).

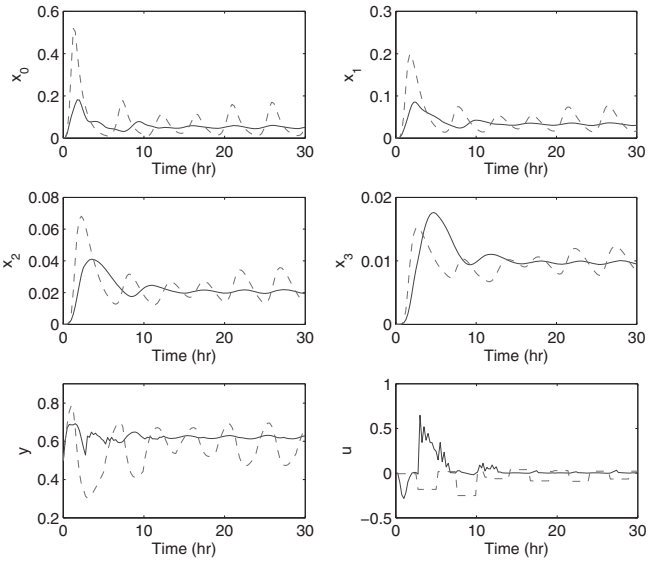

Fig. 9: State and manipulated input trajectories of Eq. (9) with PSD and solute concentration sampled asynchronously and simultaneously using the predicted manipulated input trajectory (solid curves) and the last implemented manipulated input (dashed curves) of LMPC II of Eq. (13).

5.3 Results of Asynchronous Sampling: PSD and Solute Concentration Sampled Separately

For the last set of simulations, it is assumed that one can obtain the measurements of PSD and solute concentration sampled separately. This implies that one may get a measurement of PSD at a sampling time but lack a corresponding measurement of solute concentration; or that one may have a measurement of solute concentration but lack the corresponding measurement of PSD. In addition, one can have asynchronous sampling, which means that the length of the time interval between two consecutive measurements is varying.

Using the same method as presented in section 5.2, one can generate two different time sequences $\{t^p_{k\geq 0}\}$ for PSD ($s = 2$) and $\{t^c_{k\geq 0}\}$ for solute concentration ($s = 3$) using $W^p = 0.15$ and $W^c = 1$, respectively. Both time sequences are generated with the same constraints T_{max} = 2.5 h and T_{min} = 0.25 h. The choice of $W^c = 1$ for $\{t^c_{k\geq 0}\}$ is based on the fact that one can obtain more frequent measurements of concentration. The sampling sequence $\{t^p_{k\geq 0}\}$ corresponding to the PSD measurements is shown in Figure 9, and the sampling sequence $\{t^c_{k\geq 0}\}$ corresponding to the solute concentration measurements is shown in Figure 10. Subsequently, the two sequences are merged into an ordered one $\{t_{k\geq 0}\}$ by increasing the time, and the overlapping times correspond to instants that both measurements of PSD and solute concentration can be obtained, i.e. $s = 1$. The new sequence $\{t_{k\geq 0}\}$ is shown in Figure 11. Every sampling instant in the new sequence represents a measurement of PSD or solute concentration or both. The auxiliary variable $s(t_k)$ is defined accordingly.

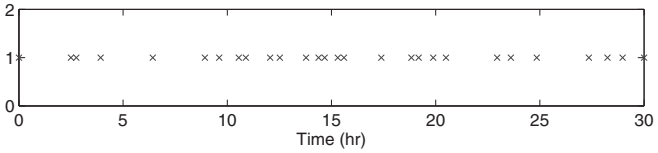

Fig. 10: Asynchronous sampling times for solute concentration.

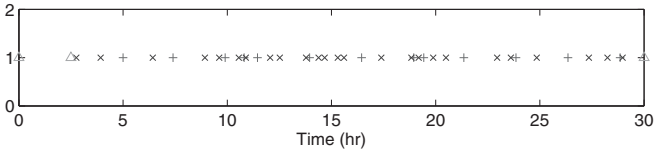

Fig. 11: Asynchronous sampling times, +: sampling times of PSD ($s(t_k) = 2$), ×: sampling times of solute concentration ($s(t_k) = 3$), Δ: sampling times of both, PSD and solute concentration ($s(t_k) = 1$).

Firstly, LMPC II is compared with MPC. The state and manipulated input trajectories are shown in Figure 12. As expected, LMPC II is able to stabilize the process, but MPC fails. This result is consistent with the previous simulations. Following that, LMPC II is compared with LMPC I. The state and manipulated input trajectories are shown in Figure 13. In this figure it can be seen that LMPC I can also stabilize the process but it takes a longer time than LMPC II. Finally, two LMPC II controllers are compared using the predicted manipulated

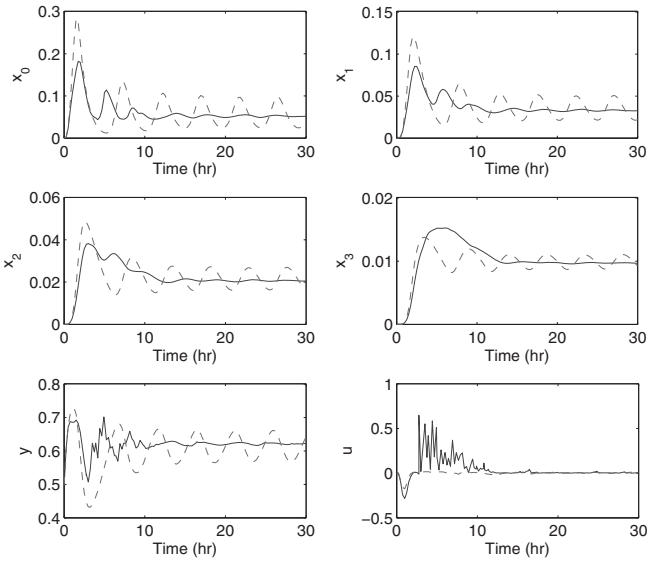

Fig. 12: State and manipulated input trajectories of Eq. (9) with PSD and solute concentration sampled asynchronously and separately using the predicted manipulated input trajectories of LMPC II of Eq. (13) (solid curves) and MPC of Eq. (10) (dashed curves).

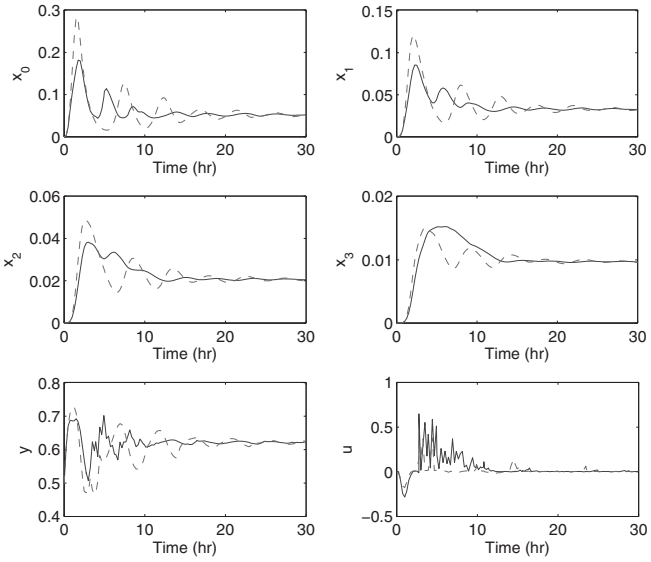

Fig. 13: State and manipulated input trajectories of Eq. (9) with PSD and solute concentration sampled asynchronously and separately using the predicted manipulated input trajectories of LMPC II of Eq. (13) (solid curves) and LMPC I of Eq. (11) (dashed curves).

input trajectory and the last implemented input, respectively. Figure 14 shows the trajectories of the state and manipulated input. This simulation demonstrates that for this case, using the last implemented manipulated input of LMPC II alone cannot stabilize the process as in the other simulations.

In this case, the overshoots of the trajectories generated by MPC and the amplitudes of oscillations of the trajectories generated by LMPC II using the last implemented manipulated input are smaller compared with the case discussed in section 5.2. This improvement is due to the decrease of the average time interval between two consecutive measurements. Despite this decrease, the performances of LMPC I and LMPC II using the predicted manipulated input trajectories do not improve much because some large intervals still exist between two consecutive measurements as shown in Figure 11.

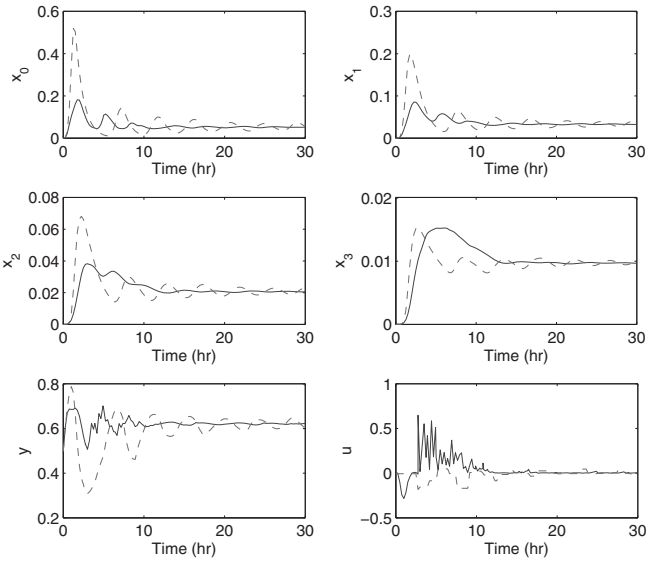

Fig. 14: State and manipulated input trajectories of Eq. (9) with PSD and solute concentration sampled asynchronously and separately using the predicted manipulated input trajectory (solid curves) and the last implemented manipulated input (dashed curves) of LMPC II of Eq. (13).

Finally, to evaluate the robustness properties of the LMPC controllers, another set of simulations was also carried out to demonstrate that LMPC II is more robust than the other two controllers when there are uncertainties in the model parameters. It is assumed that uncertainties are present in k_1 and k_2 of Eq. (9) and the actual values used to evaluate the population balance model of Eq. (9) are $1.1k_1$ and $1.1k_2$ (10 % uncertainty), which are different from the values (k_1 and k_2) used in the reduced-order moments model of Eq. (6). Figure 15 shows the results when MPC and LMPC II are applied and Figure 16 shows the results when LMPC I and LMPC II are implemented. From the two figures, it can be concluded that although LMPC II can stabilize the system, both MPC and LMPC I fail.

In summary, LMPC II using the predicted manipulated input trajectory yields a more robust closed-loop performance when the process is subject to measurement unavailability, asynchronous sampling and parametric model uncertainties.

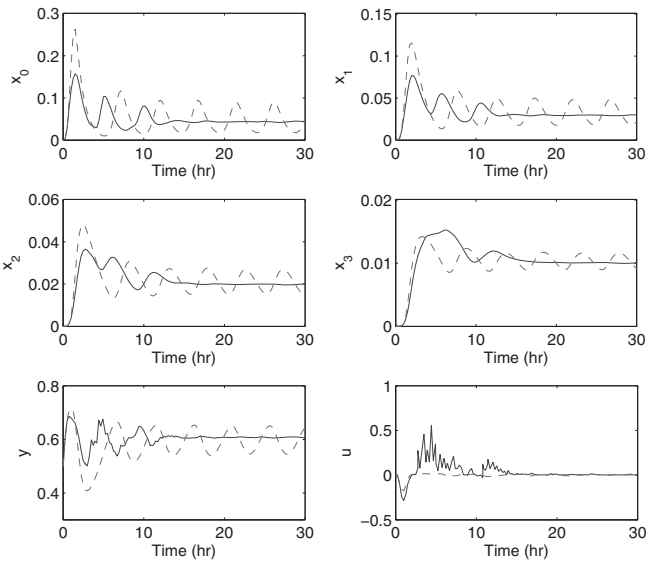

Fig. 15: State and manipulated input trajectories of Eq. (9) with 10 % uncertainty in parameters k_1 and k_2, when PSD and solute concentration are sampled asynchronously and separately using the predicted manipulated input trajectories of LMPC II of Eq. (13) (solid curves) and MPC of Eq. (10) (dashed curves).

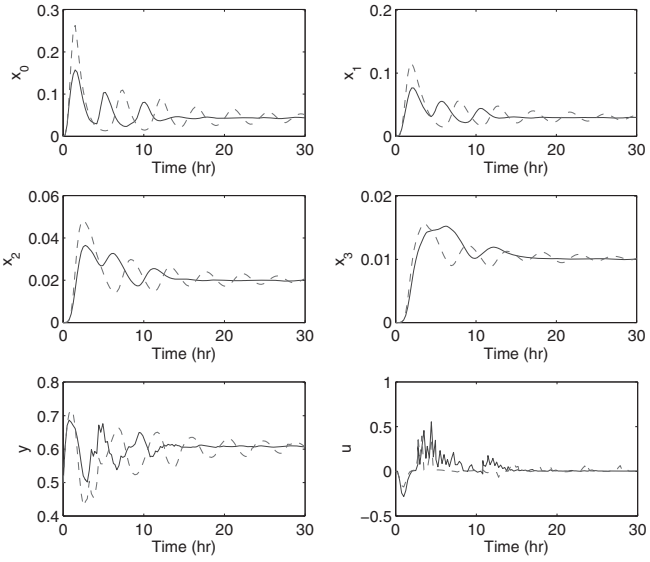

Fig. 16: State and manipulated input trajectories of Eq. (9) with 10 % uncertainty in parameters k_1 and k_2, when PSD and solute concentration are sampled asynchronously and separately using the predicted manipulated input trajectories of LMPC II of Eq. (13) (solid curves) and LMPC I of Eq. (11) (dashed curves).

6 Conclusions

In this work, the problem of controlling particulate processes described by population balance models using asynchronous measurements was considered. In particular, a continuous crystallizer was taken as an example to study the problem of preserving the closed-loop stability and robustness of a standard MPC and two recently proposed Lyapunov-based model predictive controllers, in the presence of measurement unavailability and asynchronous measurements. The simulation results demonstrate that the closed-loop system under the LMPC controller that takes possible measurement unavailability into account is more robust with respect to asynchronous measurements.

7 Acknowledgment

The financial support from NSF (Project No. CBET-0529295) is gratefully acknowledged.

8 Nomenclature

$\bar{t}$	time
χ	random variable with uniform probability distribution between 0 and 1
Δ	time elapsed since the last measurement
$\delta(r-0)$	standard Dirac function
Δ_a	interval between two consecutive sampling times
Δ_c	sampling period of model predictive controllers
Δ_m	synchronous measurement sampling time
γ	random variable with uniform probability distribution between 0 and 1
$\hat{x}(t_k)$	estimate of the state $x(t_k)$ at time t_k
μ_j	jth moment of $n(r,\bar{t})$
ρ	density of crystals
τ	residence time
$\tilde{x}_s$	unstable steady-state of the system of Eq. (5)
$\tilde{x}_v$	dimensionless moments of the crystal size distribution
x	the state of the system, defined by $x = \tilde{x} - \tilde{x}_s$
$x_L(\tau)$	sampled trajectory of Eq. (6) associated with the Lyapunov-based feedback control law h_L
$\tilde{y}$	dimensionless concentration of the solute in the crystallizer
$\{t^c_{k\geq 0}\}$	sampling time sequence of solute concentration
$\{t^p_{k\geq 0}\}$	sampling time sequence of PSD
$\{t_{k\geq 0}\}$	sampling time sequence
c	solute concentration in the crystallizer
c_0	solute concentration in the feed
c_s	concentration of solute at saturation
c_{0s}	steady-state solute concentration in the feed
$h(\Delta,\hat{x})$	control function that defines each controller
h_L	a Lyapunov-based feedback control law
k_1	positive constant appearing in the crystal growth rate

k_2 positive constant appearing in the crystal nucleation rate
k_3 positive constant appearing in the crystal nucleation rate
N prediction horizon of model predictive controllers
$n(r,\bar{t})$ the number density of crystals of radius $r\in[0,\infty)$ at time $\bar{t}$ in the suspension
P weight matrix in control Lyapunov function
p a given probability that data may be lost
$Q(\bar{t})$ crystal nucleation rate
Q_c weight matrix that defines the cost of model predictive controllers
r crystal radius
$R(\bar{t})$ crystal growth rate
R_c weight matrix that defines the cost of model predictive controllers
$S(\Delta_c)$ the family of piece-wise constant functions with sampling period Δ_c
$s(t_k)$ an auxiliary variable to indicate the available measurement at time t_k
t dimensionless time
t_k Sampling time
$T_{\max}$ the maximum time interval between two consecutive measurements
$T_{\min}$ the minimum time interval between two consecutive samplings
t_{sim} length of simulation
u dimensionless concentration of the solute in the feed
u^* optimal control actions generated by model predictive controllers
$u_{\max}$ bound on control actions
$V(x)$ a control Lyapunov function of the system of Eq. (6)
W the number of events per unit time
W^c the number of events of solute concentration sampling per unit time
W^p the number of events of PSD sampling per unit time

9 References

[1] J. B. Rawlings, S. M. Miller, W. R. Witkowski, Model identification and control of solution crystallization process. *Ind. Eng. Chem. Res.* **1993**, *32*, 1275–1296.

[2] H. M. Hulburt, S. Katz, Some problems in particle technology: A statistical mechanical formulation. *Chem. Eng. Sci.* **1964**, *19*, 555–574.

[3] D. Ramkrishna, The status of population balances. *Rev. Chem. Eng.* **1985**, *3*, 49–95.

[4] P. D. Christofides, *Model-Based Control of Particulates*, Kluwer, Dordrecht, The Netherlands, **2002**.

[5] T. Chiu, P. D. Christofides, Nonlinear control of particulate processes. *AIChE J.* **1999**, *45*, 1279–1297.

[6] A. Kalani, P. D. Christofides, Nonlinear control of spatially-inhomogeneous aerosol processes. *Chem. Eng. Sci.* **1999**, *54*, 2669–2678.

[7] T. Chiu, P. D. Christofides, Robust control of particulate processes using uncertain population balances. *AIChE J.* **2000**, *46*, 266–280.

[8] N. H. El-Farra, T. Chiu, P. D. Christofides, Analysis and control of particulate processes with input constraints. *AIChE J.* **2001**, *47*, 1849–1865.

[9] D. Shi, P. Mhaskar, N. H. El-Farra, P. D. Christofides, Predictive control of crystal size distribution in protein crystallization. *Nanotechnology* **2005**, *16*, S562–S574.

[10] D. Shi, N. H. El-Farra, M. Li, P. Mhaskar, P. D. Christofides, Predictive control of particle size distribution in particulate processes. *Chem. Eng. Sci.* **2006**, *61*, 268–281.

[11] W. Xie, S. Rohani, A. Phoenix, Dynamic modeling and operation of a seeded batch cooling crystallizer. *Chem. Eng. Commun.* **2001**, *187*, 229–249.

[12] G. P. Zhang, S. Rohani, Online optimal control of a seeded batch cooling crystallizer. *Chem. Eng. Sci.* **2003**, *58*, 1887–1896.

[13] P. Daoutidis, M. Henson, Dynamics and control of cell populations, in *AIChE Symposium Series: Proc. of 6th Intern. Conf. Chem. Proc. Contr.* (Eds.: J. B. Rawlings et al.), AIChE, New York, **2002**, pp. 274–289.

[14] F. J. Doyle, M. Soroush, C. Cordeiro, Control of product quality in polymerization processes, in *AIChE Symposium Series: Proc. of 6th Intern. Conf. Chem. Proc. Contr.* (Eds.: J. B. Rawlings et al.), AIChE, New York, **2002**, pp. 290–306.

[15] R. D. Braatz, S. Hasebe, Particle size and shape control in crystallization processes, in *AIChE Symposium Series: Proc. of 6th Intern. Conf. Chem. Proc. Contr.* (Eds.: J. B. Rawlings et al.), AIChE, New York, **2002**, pp. 307–327.

[16] P. D. Christofides, N. H. El-Farra, M. H. Li, P. Mhaskar, Model-based control of particulate processes. *Chem. Eng. Sci.* **2008**, *31*, 1156–1172.

[17] N. H. El-Farra, A. Gani, P. D. Christofides, Fault-tolerant control of process systems using communication networks. *AIChE J.* **2005**, *51*, 1665–1682.

[18] P. Mhaskar, A. Gani, N. H. El-Farra, C. McFall, P. D. Christofides, J. F. Davis, Integrated fault-detection and fault-tolerant control of process systems. *AIChE J.* **2006**, *52*, 2129–2148.

[19] P. Mhaskar, A. Gani, C. McFall, P. D. Christofides, J. F. Davis, Fault-tolerant control of nonlinear process systems subject to sensor faults. *AIChE J.* **2007**, *53*, 654–668.

[20] A. Gani, P. Mhaskar, P. D. Christofides, Handling sensor malfunctions in control of particulate processes. *Chem. Eng. Sci.* **2008**, *63*, 1217–1229.

[21] W. Zhang, M. S. Branicky, S. M. Phillips, Stability of networked control systems. *IEEE Control Syst. Mag.* **2001**, *21*, 84–89.

[22] T. C. Yang, Networked control systems: a brief survey. *IEE Proc. – Control Theory Appl.* **2006**, *153*, 403–412.

[23] H. Lin, P. J. Antsaklis, Stability and persistent disturbance attenuation properties for a class of networked control systems: switched system approach. *Int. J. Control* **2005**, *78*, 1447–1458.

[24] A. Hassibi, S. P. Boyd, J. P. How, Control of asynchronous dynamical systems with rate constraints on events. in *Proc. of the IEEE Conf. Decision Control*, Phoenix AZ, **1999**, pp. 1345–1351.

[25] G. Walsh, O. Beldiman, L. Bushnell, Asymptotic behavior of nonlinear networked control systems. *IEEE Trans. Automat. Control* **2001**, *46*, 1093–1097.

[26] D. Nešić, A. R. Teel, Input-to-state stability of networked control systems. *Automatica* **2004**, *40*, 2121–2128.

[27] L. A. Montestruque, P. J. Antsaklis, On the model-based control of networked systems. *Automatica* **2003**, *39*, 1837–1843.

[28] L. A. Montestruque, P. J. Antsaklis, Stability and persistent disturbance attenuation properties for a class of networked control systems: switched system approach. *IEEE Trans. Automat. Control* **2004**, *49*, 1562–1572.

[29] W. J. Kim, K. Ji, A. Ambike, Networked real-time control strategy dealing with stochastic time delays and packet losses. *ASME J. Dyn. Syst. Meas. Control* **2006**, *128*, 681–685.

[30] W. J. Kim, K. Ji, A. Srivastava, Network-based control with real-time prediction of delayed/lost sensor data. *IEEE Trans. Control Syst. Technol.* **2006**, *14*, 182–185.

[31] P. Mhaskar, N. H. El-Farra, P. D. Christofides, Predictive control of switched nonlinear systems with scheduled mode transitions. *IEEE Trans. Automat. Control* **2005**, *50*, 1670–1680.

[32] P. Mhaskar, N. H. El-Farra, P. D. Christofides, Stabilization of Nonlinear Systems with State and Control Constraints Using Lyapunov-Based Predictive Control. *Syst. & Contr. Lett.* **2006**, *55*, 650–659.

[33] D. Muñoz de la Peña, P. D. Christofides, Lyapunov-Based Model Predictive Control of Nonlinear Systems Subject to Data Losses. *IEEE Trans. Autom. Contr.* **2008**, *53*, 2076–2098.

[34] S. J. Lei, R. Shinnar, S. Katz, The stability and dynamic behavior of a continuous crystallizer with a fines trap. *AIChE J.* **1971**, *17*, 1459–1470.

[35] G. R. Jerauld, Y. Vasatis, M. F. Doherty, Simple conditions for the appearance of sustained oscillations in continuous crystallizers. *Chem. Eng. Sci.* **1983**, *38*, 1675–1681.

[36] P. Kokotovic, M. Arcak, Constructive nonlinear control: a historical perspective. *Automatica* **2001**, *37*, 637–662.

[37] P. D. Christofides, N. H. El-Farra, *Control of Nonlinear and Hybird Process Systems: Designs for Uncertainty, Constraints and Time-Delays*, Springer-Verlag, Berlin, **2005**.

[38] Y. Lin, E. D. Sontag, A universal formula for stabilization with bounded controls. *Syst. Control Lett.* **1991**, *16*, 393–397.

[39] N. H. El-Farra, P. D. Christofides, Integrating robustness, optimality and constraints in control of nonlinear processes. *Chem. Eng. Sci.* **2001**, *56*, 1841–1868.

[40] N. H. El-Farra, P. D. Christofides, Bounded robust control of constrained multivariabe nonlinear processes. *Chem. Eng. Sci.* **2003**, *58*, 3025–3047.

[41] C. E. García, D. M. Prett, M. Morari, Model predictive control: Theory and practice – a survey. *Automatica* **1989**, *25*, 335–348.

